

# Vortex-induced vibration of a slender single-span cylinder

N. Oikou

Delft University of Technology, the Netherlands

The goal of this paper is to study the vortex-induced vibration of slender cylindrical structures. For this purpose, a 2D model that calculates the coupled cross-flow and in-line vibrations of a flexible single span beam is developed. A wake oscillator known to match well with free vibration experiments on rigid elastically mounted cylinders is employed for the description of the vortex forces acting on the pipe. The frequency of the oscillating beam is determined from the Fourier spectrum of the analysed time series and is presented, together with the maximum oscillating amplitudes over a range of flow velocities. The model is compared with measurements from experiments and good agreement is found.

*Key words: Vortex-induced vibration, non-linear dynamics, wake oscillator, fluid-structure interaction, floating pipeline*

## 1 Introduction

As a fluid flow meets a bluff body such as a cylindrical beam, the flow separates and vortices are formed. In the case of a stationary rigid cylinder, the frequency of vortex shedding increases linearly with flow velocity obeying the so-called Strouhal law. The alternate shedding of vortices generates forces on the beam. In the case of an elastically mounted rigid cylinder, these forces might lead to large amplitude vibration as the shedding frequency approaches the natural frequency of the cylinder. A further increase of the flow velocity does not increase the shedding frequency, but it locks into the natural frequency of the cylinder for a range of flow velocities. The phenomenon is known as vortex-induced vibration and it might cause problems in long cylindrical structures such as pipelines, long chimneys and bridge cables. For a review on vortex-induced vibration see Sarpkaya (2004) and Williamson et al. (2004).

In this paper we study the response of a flexible tensioned cylindrical beam placed in a stationary uniform flow. The near wake vortex street is modelled by a continuous

distribution of wake oscillators arranged along the cylinder length. Wake oscillator models have been applied in the study of flexible structures before, see Mathelin et al. (2005) and Violette et al. (2007), however lacking experimental validation. Ogink et al. (2010) improved a model for the prediction of vortex-induced vibration on an elastically mounted rigid cylinder in fluid flow developed by Facchinetti et al. (2004), by taking into account the relative velocity between the flow and the cylinder motion. Their model was shown to be able to tune easily to either the upper or lower branch of the free vibration experiments such as those performed by Khalak et al. (1999). In this work we extend the couple wake-cylinder model developed by Ogink et al. in order to simulate vortex-induced vibration on long flexible cylinders, accounting for the relative velocity between the flow and the cylinder motion. The model is compared to the measurements of Tsahalis (1984) and is shown to yield realistic results.

## 2 Mathematical modelling of slender single-span cylinders

### 2.1 Force decomposition

Consider a straight cylindrical beam with diameter  $D$  and length  $L$ , as shown in Figure 1. The cylinder is pinned on both ends and is placed in a uniform stationary fluid flow with velocity  $V$ . Let  $x$  denote the in-line direction with respect to the incoming flow,  $y$  the cross-flow direction and  $z$  the direction along the cylinder. Let  $w_x(z,t)$  and  $w_y(z,t)$  be the displacements of a cylinder with respect to the equilibrium position due to the interaction with the flow, with  $t$  denoting the time.

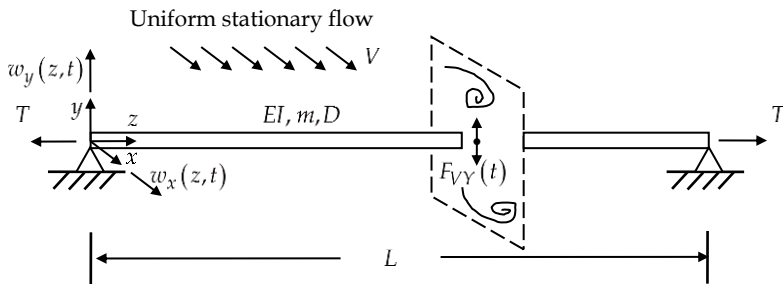


Figure 1: Sketch of a slender beam in uniform stationary flow

Assume that the beam moves in the  $x-y$  plane and that its length and the wavelength of its deformation are large compared to its diameter, so that the Euler-Bernoulli theory is applicable for the bending of the beam. With these assumptions, the equations that govern the horizontal and vertical motion of a differential element of the cylinder can be written as

$$(m + m_a) \frac{\partial^2 w_x}{\partial t^2} + b \frac{\partial w_x}{\partial t} + EI \frac{\partial^4 w_x}{\partial z^4} - T \frac{\partial^2 w_x}{\partial z^2} = F_{VX}, \quad (1)$$

$$(m + m_a) \frac{\partial^2 w_y}{\partial t^2} + b \frac{\partial w_y}{\partial t} + EI \frac{\partial^4 w_y}{\partial z^4} - T \frac{\partial^2 w_y}{\partial z^2} = F_{VY}, \quad (2)$$

in which  $m$  is the cylinder mass per unit length,  $m_a$  is the potential added mass per unit length,  $b$  is the structural damping,  $EI$  is the cylinder bending stiffness,  $T$  is the axial tension on the beam and  $F_{VX}$ ,  $F_{VY}$  are the in-line and cross-flow forces per unit length that are exerted on the beam due to the vortex shedding. The added mass  $m_a$  is given by  $m_a = 1/4 C_a \pi \rho D^2$ , where  $\rho$  is the fluid density and  $C_a$  is the potential added mass coefficient. The boundary conditions for the simply supported beam are given by

$$w_x(0) = w_x(L) = EI \frac{\partial^2 w_x(0)}{\partial z^2} = EI \frac{\partial^2 w_x(L)}{\partial z^2} = 0, \quad (3)$$

$$w_y(0) = w_y(L) = EI \frac{\partial^2 w_y(0)}{\partial z^2} = EI \frac{\partial^2 w_y(L)}{\partial z^2} = 0. \quad (4)$$

We decompose the relative velocity  $U$  of the fluid with respect to the cylinder motion as  $U_x = V - dw_x/dt$  and  $U_y = -dw_y/dt$ , see Figure 2. We define the angle  $\beta$  between the directions of  $U_x$  and  $U$ , also shown in Figure 2, as

$$\sin \beta = U_y / U = -\frac{dw_y}{dt} / \sqrt{\left(V - \frac{dw_x}{dt}\right)^2 + \left(\frac{dw_y}{dt}\right)^2}, \quad (5)$$

$$\cos \beta = U_x / U = \left(V - \frac{dw_x}{dt}\right) / \sqrt{\left(V - \frac{dw_x}{dt}\right)^2 + \left(\frac{dw_y}{dt}\right)^2}. \quad (6)$$

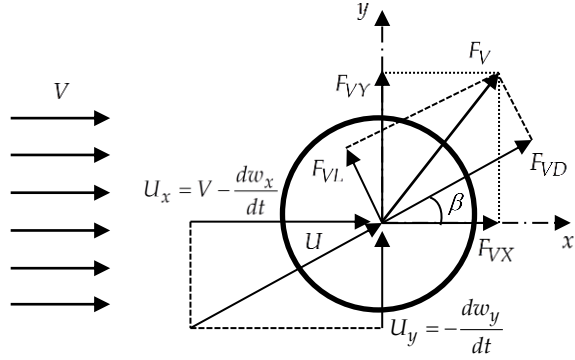


Figure 2: Illustration of the relative velocity of the flow with respect to the cylinder motion and of the vortex fluid forces exerted on a cross-section of the cylinder

Next, we follow Ogink (2010) and we decompose the vortex forces  $F_{VX}$  and  $F_{VY}$  in a lift part  $F_{VL}$  perpendicular to and a drag part  $F_{VD}$  in-line with the relative velocity  $U$ , as

$$F_{VX} = F_{VD} \cos \beta - F_{VL} \sin \beta, \quad (7)$$

$$F_{VY} = F_{VD} \sin \beta + F_{VL} \cos \beta. \quad (8)$$

Using the dimensionless expressions  $C_{VD} = F_{VD} / \left( \frac{1}{2} \rho D U^2 \right)$  and  $C_{VL} = F_{VL} / \left( \frac{1}{2} \rho D U^2 \right)$ , the vortex forces  $F_{VX}$  and  $F_{VY}$  can be expressed as

$$F_{VX} = \frac{1}{2} \rho D U^2 (C_{VD} \cos \beta - C_{VL} \sin \beta), \quad (9)$$

$$F_{VY} = \frac{1}{2} \rho D U^2 (C_{VD} \sin \beta + C_{VL} \cos \beta). \quad (10)$$

Following Facchinetti et al. (2004), we associate the vortex lift force coefficient  $C_{VL}$  with a wake variable  $q$  that obeys a Van der Pol differential equation, able to model the lock-in of the vortex lift force when coupled with the structural motion, as

$$C_{VL} = \frac{C_{y1}}{q_1} q. \quad (11)$$

Here  $C_{y1}$  is the oscillating cross-flow force measured on a rigid stationary cylinder and  $q_1$  is the amplitude of the limit cycle of the unforced wake oscillator, in our case  $q_1 = 2$ . The vortex drag force  $C_{VD}$  is associated with the mean in-line force  $C_{x0}$  measured on a rigid stationary cylinder, as

$$C_{VD} = C_{x0}. \quad (12)$$

Facchinetti et al. compared a structural displacement, velocity and acceleration coupling, and showed that the latter is dominant in the description of the cylinder forcing on the wake oscillator. In these lines, an appropriate selection for a distributed wake oscillator able to describe the cross flow force along the cylinder is given by

$$\frac{\partial^2 q}{\partial t^2} - \varepsilon \omega_s (1 - q^2) \frac{\partial q}{\partial t} + \omega_s^2 q = \frac{A}{D} \frac{\partial^2 w_y}{\partial t^2}, \quad (13)$$

where  $\varepsilon$ ,  $A$  are tuning parameters for the model and  $\omega_s$  is the Strouhal angular frequency given by  $\omega_s = 2\pi St V/D$ , where  $St$  is the Strouhal number.

## 2.2 Dimensionless form of equations of motion

Introducing the following dimensionless variables and parameters

$$\begin{aligned} \tilde{w}_x &= w_x/D, \quad \tilde{w}_y = w_y/D, \quad \tilde{x} = x/D, \quad \tilde{y} = y/D, \quad \tilde{z} = z/D, \quad \tau = \omega_s t, \quad \zeta = b/(2\omega_s(m+m_a)), \\ \kappa &= EI/(D^4\omega_s^2(m+m_a)), \quad \lambda = T/(D^2\omega_s^2(m+m_a)) \quad \text{and} \quad m^* = 4m/(\pi\rho D^2), \end{aligned}$$

we can express Eqs. (1), (2) and (13) that govern the horizontal and vertical motion of a differential element of the beam in dimensionless form as

$$\frac{\partial^2 \tilde{w}_x}{\partial \tau^2} + 2\zeta \frac{\partial \tilde{w}_x}{\partial \tau} + \kappa \frac{\partial^4 \tilde{w}_x}{\partial \tilde{z}^4} - \lambda \frac{\partial^2 \tilde{w}_x}{\partial \tilde{z}^2} = \frac{1}{m^* + C_a} \frac{1}{2\pi^3 St^2} C_{VX}, \quad (14)$$

$$\frac{\partial^2 \tilde{w}_y}{\partial \tau^2} + 2\zeta \frac{\partial \tilde{w}_y}{\partial \tau} + \kappa \frac{\partial^4 \tilde{w}_y}{\partial \tilde{z}^4} - \lambda \frac{\partial^2 \tilde{w}_y}{\partial \tilde{z}^2} = \frac{1}{m^* + C_a} \frac{1}{2\pi^3 St^2} C_{VY}, \quad (15)$$

$$\frac{\partial^2 q}{\partial \tau^2} - \varepsilon(1-q^2) \frac{\partial q}{\partial \tau} + q = A \left( \frac{\partial^2 y}{\partial \tau^2} \cos \beta + \frac{\partial^2 x}{\partial \tau^2} \sin \beta \right), \quad (16)$$

where the in-line and cross-flow vortex force coefficients  $C_{VX}$  and  $C_{VY}$  are given by

$$C_{VX} = \left( \left( 1 - 2\pi St \frac{d\tilde{w}_x}{d\tau} \right) C_{VD} + 2\pi St \frac{d\tilde{w}_y}{d\tau} C_{VL} \right) \sqrt{\left( 1 - 2\pi St \frac{d\tilde{w}_x}{d\tau} \right)^2 + \left( 2\pi St \frac{d\tilde{w}_y}{d\tau} \right)^2}, \quad (17)$$

$$C_{VY} = \left( -2\pi St \frac{d\tilde{w}_y}{d\tau} C_{VD} + \left( 1 - 2\pi St \frac{d\tilde{w}_x}{d\tau} \right) C_{VL} \right) \sqrt{\left( 1 - 2\pi St \frac{d\tilde{w}_x}{d\tau} \right)^2 + \left( 2\pi St \frac{d\tilde{w}_y}{d\tau} \right)^2}. \quad (18)$$

The angle  $\beta$  can be expressed in dimensionless form as

$$\sin \beta = -2\pi St \frac{d\tilde{w}_y}{d\tau} / \sqrt{\left( 1 - 2\pi St \frac{d\tilde{w}_x}{d\tau} \right)^2 + \left( 2\pi St \frac{d\tilde{w}_y}{d\tau} \right)^2}, \quad (19)$$

$$\cos \beta = \left( 1 - 2\pi St \frac{d\tilde{w}_x}{d\tau} \right) / \sqrt{\left( 1 - 2\pi St \frac{d\tilde{w}_x}{d\tau} \right)^2 + \left( 2\pi St \frac{d\tilde{w}_y}{d\tau} \right)^2}. \quad (20)$$

Finally, the boundary conditions can be expressed in dimensionless form as

$$\tilde{w}_x(0) = \tilde{w}_x(L/D) = \frac{\partial^2 \tilde{w}_x(0)}{\partial \tilde{z}^2} = \frac{\partial^2 \tilde{w}_x(L/D)}{\partial \tilde{z}^2} = 0, \quad (21)$$

$$\tilde{w}_y(0) = \tilde{w}_y(L/D) = \frac{\partial^2 \tilde{w}_y(0)}{\partial \tilde{z}^2} = \frac{\partial^2 \tilde{w}_y(L/D)}{\partial \tilde{z}^2} = 0. \quad (22)$$

### 2.3 Cylinder natural frequencies and natural modes

The natural frequencies of the cylinder in water are identical for the in-line and the cross-flow direction, due to the symmetry of the problem, and can be calculated using the formula

Table 1: Natural frequencies of the cylinder

Frequency	$\omega_n$ [rad/s]	Frequency	$\omega_n$ [rad/s]	Frequency	$\omega_n$ [rad/s]
1	0.6305	4	2.7838	7	5.7527
2	1.2882	5	3.6622	8	6.9844
3	1.9986	6	4.6481	9	8.3493

$$f_n = \frac{\omega_n}{2\pi} = \frac{1}{2\pi} \sqrt{\frac{EI}{m+m_a} \left( -\left(\frac{T}{2EI}\right)^2 + \left( \left(\frac{\pi n}{L}\right)^2 + \frac{T}{2EI} \right)^2 \right)}, \quad n=1,2,3,\dots \quad (23)$$

where  $f_n$  and  $\omega_n$  represent the  $n$ th natural and angular natural frequency of the cylinder, respectively. The system properties are chosen as

$$D = 0.0254 \text{ m}, \quad L = 8 \text{ m}, \quad m = 0.524 \text{ kg/m}, \quad m_a = 0.507 \text{ kg/m}, \quad EI = 0.255 \text{ Nm}^2,$$

$$T = 2.64 \text{ N}, \quad \zeta = 0.001.$$

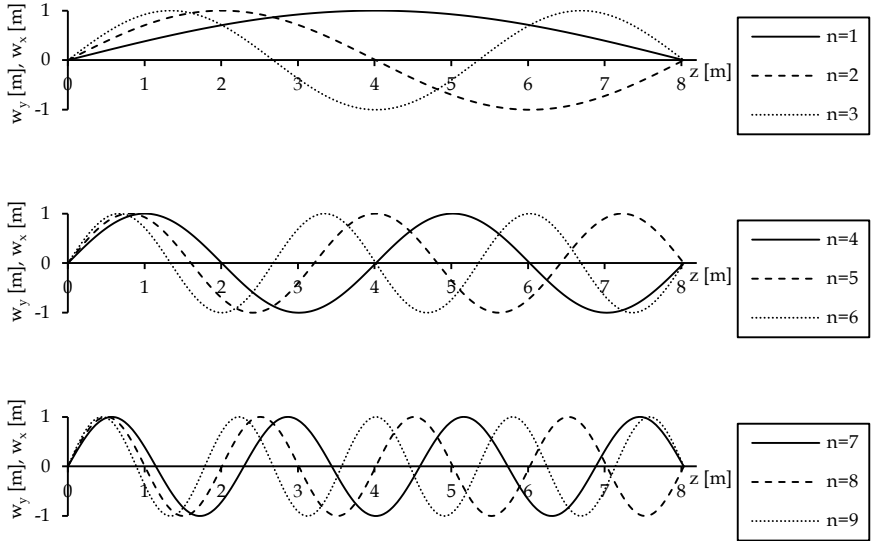


Figure 3: Normal mode shapes of the cylinder

and correspond to a PVC cylinder. The first nine natural frequencies of the cylinder are presented in Table 1. The corresponding natural modes of the cylinder oscillation are calculated using the formula

$$w_{y,n}(z) = w_{x,n}(z) = \sin \left[ \frac{1}{2} \left( \frac{2T}{EI} + 2 \sqrt{\frac{T^2}{EI^2} + \frac{4(m+m_a)\omega_n^2}{EI}} \right) z \right], \quad z \in [0, L], \quad n = 1, 2, 3, \dots \quad (24)$$

and are presented in Figure 3. For a derivation of Eqs. (23)-(24), see Bokaian (1990).

### 3 Numerical implementation and discussion

The coupled system of partial differential equations (14) - (16) was solved numerically in Fortran by approximating the spatial derivatives with a second order finite difference scheme and integrating the resulting set of ordinary differential equations in time using a fifth order Runge-Kutta scheme. The spatial discretization was chosen as  $\Delta z = 0.05$  m and the time step was equal to  $\Delta \tau = T_s/100$ , where  $T_s$  stands for the period of the Strouhal frequency. The initial conditions were chosen as

$$\tilde{w}_y = 0, \quad d\tilde{w}_y/d\tilde{z} = 0, \quad \tilde{w}_x = 0, \quad d\tilde{w}_x/d\tilde{z} = 0, \quad q = 0.1 \quad \text{and} \quad dq/d\tilde{z} = 0.$$

The values for  $C_{x0}$ ,  $C_{y1}$ ,  $St$  were taken from the measurements of Gopalkrishnan (1993) on stationary cylinders and are equal to  $C_{x0} = 1.1856$ ,  $C_{y1} = 0.3842$  and  $St = 0.1932$ . The potential added mass coefficient  $C_a$  is equal to 1 and the tuning parameters of the wake oscillator are chosen as  $\varepsilon = 0.7$ ,  $A = 12$ .

The mean displacement in the  $x$  direction was calculated from a time series with a length of 100 periods. The maximum recurrent cross-flow and in-line displacement at a given position along the cylinder was found from a time series with a length of 100 periods and the oscillating frequency  $\omega_c$  was determined by the highest peak in the Fourier spectrum of the analysed time series. The calculation was repeated over a range of flow velocities in order to search for lock-in over higher natural frequencies of the cylinder.



All calculations were performed twice, in order to search for hysteresis, once where the initial conditions were equal to the last lower flow velocity and once in backward direction, where the initial conditions were equal to the last higher flow velocity. The steady state was typically reached after 50 periods of oscillation. The model results were verified by comparing them to a numerical solution using modal superposition and good agreement between the two solutions was found.

The cross-flow and in-line displacements along the cylinder at a maximum of the cross-flow amplitude are shown in Figure 4 for  $V=0.09$  m/s. This velocity corresponds to a Strouhal frequency equal to 4.3 rad/s. The cross-flow amplitude resembles the fifth mode shape of the cylinder. As shown in Figure 5, the cross-flow vibration occurs at a frequency equal to 3.69 rad/s, close its fifth natural frequency. The circles in the frequency spectra denote the natural frequencies of the cylinder in the shown range. The vortex lift force oscillates at the exact same frequency, which means that the vortex-shedding is synchronized to the vibration frequency, not obeying the Strouhal law. This is in agreement with observations on vortex-induced vibrations of one-degree of freedom rigid elastically mounted cylinders, see for example Gopalkrishnan (1993).

The mean displacement in the in-line direction at  $z = 4$  m is equal to  $18D$ , a relatively high value, probably due to the low bending stiffness of the cylinder. The maximum in-line vibration amplitude at the same location is less than  $0.1D$ , hence it can be hardly seen in Figure 5 (middle, left). It can be also observed that the in-line vibration frequency is 7.38 rad/s, twice as much as the cross-flow vibration frequency. This results in the characteristic figure-eight trajectory, which can be seen in Figure 6 for two different locations along the cylinder, close to two of the antinodes of its fifth mode shape.

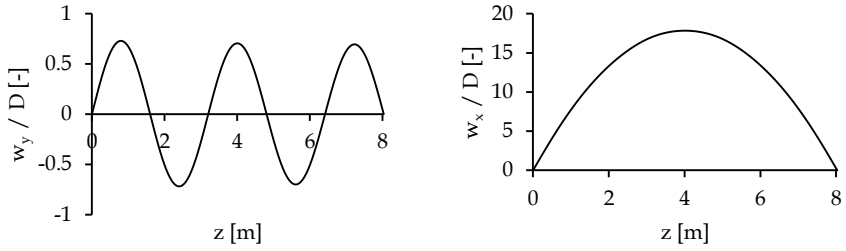


Figure 4: Cross-flow (left) and in-line (right) displacement at a maximum of the steady-state response for  $V=0.09$  m/s

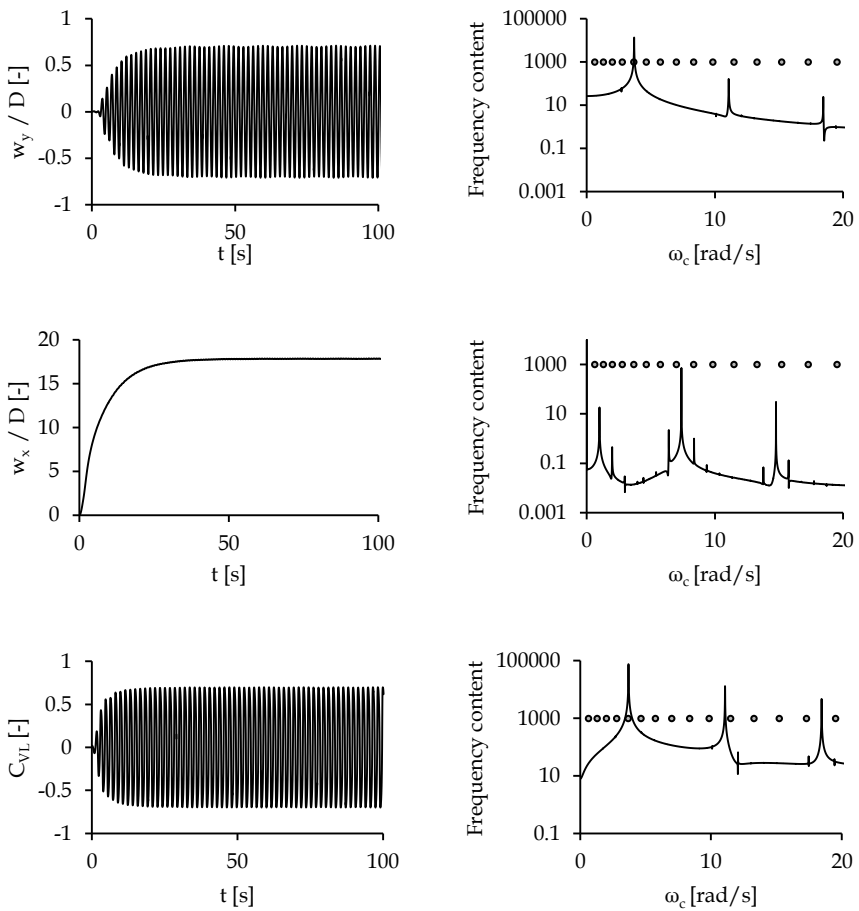


Figure 5: Time series and Fourier spectrum of the cross-flow oscillation (upper part), the in-line oscillation (middle part) and the vortex lift force (lower part), at the midpoint of the cylinder

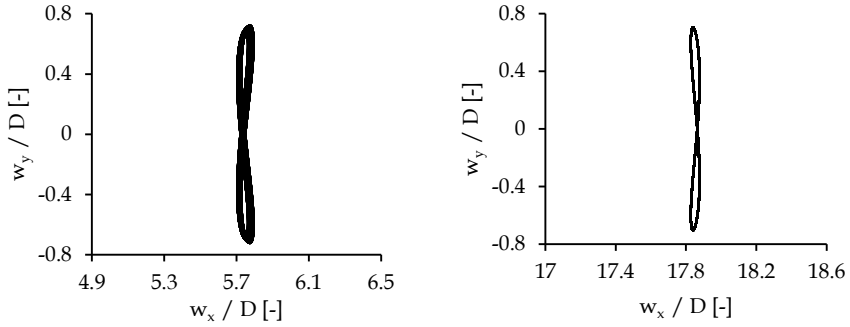


Figure 6: Trajectory of vibration at  $z = 1.6$  m (left) and  $z = 4$  m (right)

Next, the maximum response of the cylinder is sought over a range of flow velocities. The system is solved in the range  $V = 0.005 - 0.1$  m/s with a velocity step equal to  $0.0025$  m/s. In the graphs that follow, solid lines correspond to increasing velocities, dashed lines correspond to decreasing velocities and circles denote the natural frequencies of the cylinder. The dotted lines represent the Strouhal frequency  $\omega_s$  and twice the Strouhal frequency  $2\omega_s$ , in the cross-flow and in-line plots respectively. Figure 7 shows the maximum calculated amplitude and frequency of cross-flow oscillation at the midpoint of the cylinder. The cylinder locks into the first natural frequency of the cylinder in the range  $V = 0.01 - 0.02$  m/s, into the third one in the range  $V = 0.04 - 0.06$  m/s and into the fifth one in the range  $V = 0.08 - 0.1$  m/s. The amplitude of the motion in the lock-in ranges is around  $0.7D$ . The fact that the cylinder locks into the odd-numbered natural frequencies of the cylinder can be understood by looking at the shape of the natural modes. At the midpoint of the beam the even-numbered natural modes have a node and they do not contribute much compared to the odd-numbered modes.

In Figure 8, the maximum vibration amplitude and frequency in the in-line direction is shown for the same range of flow velocities. The in-line vibration amplitude is found to be around  $0.05D$  and the cylinder is now seen to be locked in one of its natural frequencies for all flow velocities. This is probably due to the fact that its natural frequencies are closely spaced and the lock-in ranges overlap with each other.

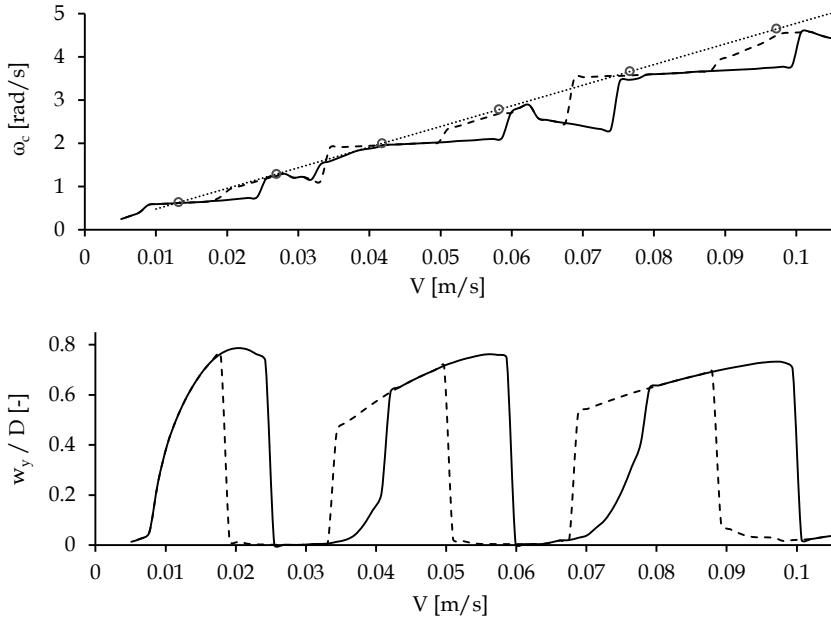


Figure 7: Frequency (upper part) and amplitude (lower part) of the cross-flow oscillation at the midpoint of the cylinder

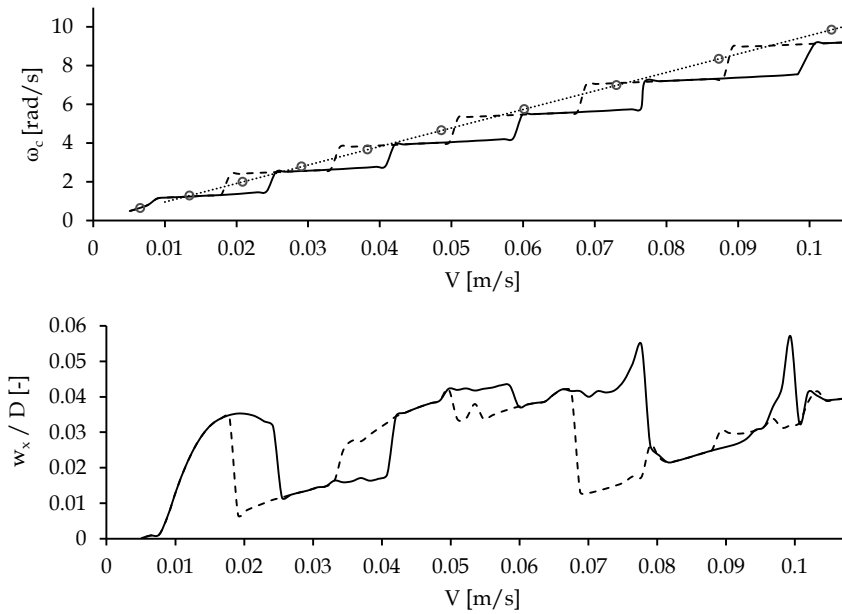


Figure 8: Frequency (upper part) and amplitude (lower part) of the in-line oscillation at the midpoint of the cylinder

## 4 Comparison to experiment

Experiments on vortex-induced vibration focus on simple cases of short rigid cylinders in 2D flow and few studies consider flexible pipes. Here the model is compared to the free vibration experiments of Tsahalis (1984). In his experiments a cylinder was placed in a water channel and allowed to vibrate in both the cross-flow and the in-line direction for different flow velocities. The properties corresponding to his experimental setup were

$$D = 0.019 \text{ m}, L = 2.14 \text{ m}, m = 0.6416 \text{ kg/m}, m_a = 0.2835 \text{ kg/m}, EI = 77.82 \text{ Nm}^2, \\ T = 0 \text{ N}, \omega_{n1} = 19.77 \text{ rad/s}, \zeta = 0.0159.$$

In Figure 9, the RMS value of the amplitude and frequency of the steady state response of the cross-flow oscillation, predicted by the model for this set of parameters is compared to the measurements of Tsahalis for a range of flow velocities. His measurements represent the lock-in behaviour of the first mode only. Over this range a good agreement is found with the model prediction.

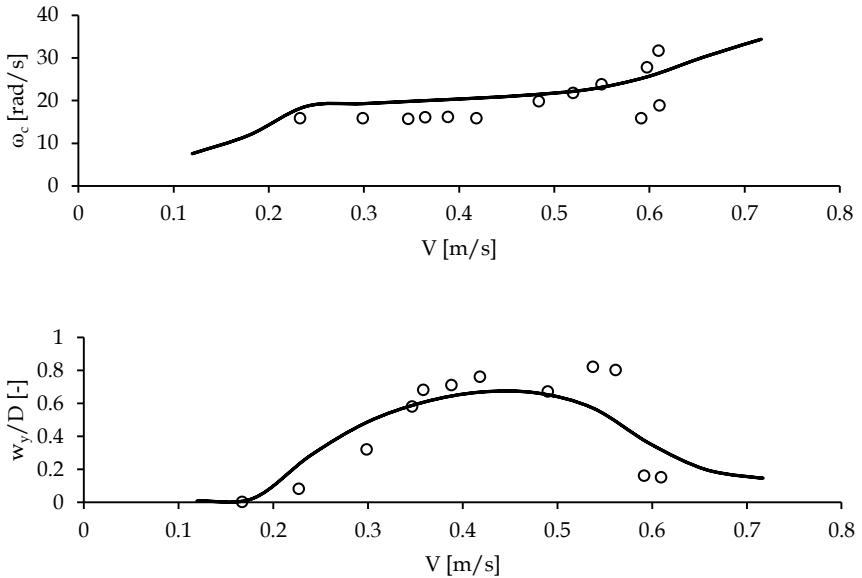


Figure 9: Frequency (upper part) and RMS amplitude (lower part) of the cross-flow oscillation at the midpoint of the cylinder. Circles: Measurements of Tsahalis (1984), Solid line: Model prediction

## 5 Conclusions

In this work we extended an existing wake-cylinder model in order to study the response of a free spanning cylindrical beam subject to a uniform stationary flow. The model does not require any a priori assumptions about the frequency and the mode of vibration, making it possible to predict multimode excitation. The frequency spectra of the cross-flow oscillation at the midpoint of the cylinder show that vibration occurs in well-defined frequency bands for certain lock-in velocity ranges, in which the vortex shedding is synchronized to the frequency of the cross-flow vibration, not obeying the Strouhal law. In the same velocity range, the in-line vibration frequency is found to be double the frequency of the cross-flow oscillation and the cylinder trajectory follows the characteristic figure-eight pattern. The model is compared to free vibration measurements on flexible horizontal cylinders and good agreement is found.

The coupled wake-oscillator model is faster and easier to apply compared to the Computational Fluid Dynamics (CFD) models and is more effective in modelling vortex-induced vibration than single variable models. The model can be easily extended to model multi-span and variable tension (vertical) long cylindrical structures prone to vortex-induced vibration.

## Literature

- Bokaian, A. (1990). Natural frequencies of beams under tensile axial loads. *Journal of Sound and Vibration*, 142(3), 481-498.
- Facchinetti, M. L., de Langre, E., & Biolley, F. (2004). Coupling of structure and wake oscillators in vortex-induced vibrations. *Journal of Fluids and Structures*, 19(2), 123-140.
- Gopalkrishnan, R. (1993). *Vortex-induced forces on oscillating bluff cylinders*. Ph.D. thesis, Massachusetts Institute of Technology.
- Khalak, A., & Williamson, C. H. K. (1999). Motions, forces and mode transitions in vortex-induced vibrations at low mass-damping. *Journal of Fluids and Structures*, 13(7), 813-851.
- Mathelin, L., & De Langre, E. (2005). Vortex-induced vibrations and waves under shear flow with a wake oscillator model. *European Journal of Mechanics-B/Fluids*, 24(4), 478-490.

- Ogink, R. H. M., & Metrikine, A. V. (2010). A wake oscillator with frequency dependent coupling for the modeling of vortex-induced vibration. *Journal of Sound and Vibration*, 329(26), 5452-5473.
- Sarpkaya, T. (2004). A critical review of the intrinsic nature of vortex-induced vibrations. *Journal of Fluids and Structures*, 19(4), 389-447.
- Tsahalis, D. T. (1984). Vortex-induced vibrations of a flexible cylinder near a plane boundary exposed to steady and wave-induced currents. *Journal of Energy Resources Technology*, 106(2), 206-213.
- Violette, R., De Langre, E., & Szydlowski, J. (2007). Computation of vortex-induced vibrations of long structures using a wake oscillator model: Comparison with DNS and experiments. *Computers & Structures*, 85(11), 1134-1141.
- Williamson, C. H. K., & Govardhan, R. (2004). Vortex-induced vibrations. *Annu. Rev. Fluid Mech.*, 36, 413-455.